Journal of Environmental Chemical Engineering 7 (2019) 102815

Contents lists available at ScienceDirect

Journal of Environmental Chemical Engineering

journal homepage: www.elsevier.com/locate/jece

Precipitation of a layered double hydroxide comprising Mg^{2+} and Al^{3+} to remove sulphate ions from aqueous solutions

Damaris Guimarães*, Natasha C.M. da Rocha, Rafaela A.P. de Morais, Andréia De-Lazzari B.P. Resende, Rosa M.F. Lima, Geraldo M. da Costa, Versiane A. Leão

Federal University of Ouro Preto, Campus Morro do Cruzeiro, s.n., Bauxita, Ouro Preto, MG, 35400-000, Brazil

ARTICLE INFO

Keywords:
Sulphate removal
Precipitation
Layered double hydroxide
Characterisation
Wastewater treatment

ABSTRACT

This work presents an alternative route to remove sulphate ions from aqueous solutions, which is simple and fast, and its efficiency of sulphate removal is slightly influenced by temperature (26 °C–70 °C) and pH (4–12). The lowest residual sulphate concentration was about 60 mg L^{-1}, which was observed in continuous experiments using wastewater (26 °C, pH 6 and initial sulphate concentration of 630 mg L^{-1}). All these outcomes together have not been observed in the current most used processes of sulphate precipitation, i.e. gypsum and ettringite precipitation. Sulphate removal experiments were carried out in the batch and continuous systems using synthetic solutions. In these conditions, about 75% of sulphate ions were removed for an initial ion concentration of 1800 mg L^{-1}. A continuous test was also performed using a wastewater sample in addition to a synthetic solution. The system reached steady-state conditions after four residence times (40 min) in the experiment with synthetic solutions, whereas three residence times (30 min) were necessary for the tests with the wastewater (initial sulphate concentration of 630 mg L^{-1}). In the latter case, the sulphate removal efficiency was approximately 90%. The characterisation of the experimentally precipitated solids was carried out by DRX, FTIR, SEM-EDS, elemental analysis and thermal analysis. These techniques showed that, except in pH 4, the sulphate removal process occurred due to the precipitation of a layered double hydroxide, comprising Mg^{2+} and Al^{3+} as its metallic ions and nitrate (due to the salts used for precipitation) and sulphate anions occupying its interlayer space.

1. Introduction

Currently, the removal of sulphate ions from aqueous solutions represents a great challenge to several applications, such as petrol exploration and tanning, cellulose, fertiliser, mining and textile industries. In their processes, such industries use raw materials which contain different forms of sulphur in any of its oxidation states, and therefore, effluents rich in sulphate under oxidizing conditions are often produced [1,2].

The presence of sulphate ions in process waters causes corrosion of pipes, structures and equipment composed of different materials. Besides, from the moment when high sulphate content wastewaters are released in the environment, they account for environmental impacts such as the increase in the content of dissolved salts in aqueous systems [3–5]. According to the World Health Organization (WHO), the organoleptic properties of drinking waters are altered when the sulphate content is higher than 500 mg L^{-1}, which may cause serious cases of diarrhoea and dehydration to human beings and animals [6].

Due to the risks to the human population and also to the environment, wastewaters with a high sulphate content need to comply with the environmental policies of each country as well as with the WHO recommendations [6]. Among the techniques applied to treat this type of effluent, precipitation is the most important of them. Generally, it is preceded by acidity neutralisation, followed by precipitation of gypsum [7–11] or ettringite [12–16].

In general, among the precipitation routes for removal of anions from aqueous solutions, an important class of compounds, i.e. layered double hydroxides (LDHs) has received considerable attention in recent years [17–22]. The general chemical formula of these compounds may be represented as:

$$[M^{2+}_{(1-X)}M^{3+}_{(X)}(OH)_2]^{X+}(A^{m-})_{(X/m)}\cdot nH_2O$$

In which, M^{2+} and M^{3+} are divalent and trivalent ions, respectively, A^{m-} is the compensation anion, with the charge m−, n is the number of water molecules located in the interlayer space, and X is the relation

* Corresponding author.
E-mail address: guimaraes.damaris@yahoo.com.br (D. Guimarães).

https://doi.org/10.1016/j.jece.2018.102815
Received 19 August 2018; Received in revised form 4 November 2018; Accepted 1 December 2018
Available online 03 December 2018

$M^{3+}/[M^{2+} + M^{3+}]$, which may assume values from 0.1 to 0.33 [23].

Since a wide variety of LDHs can be formed by different metals and anions, they have received great attention in studies focusing on the treatment of effluents containing organic and inorganic species, for instance, fatty acids, oxyanions and halides [17–22]. However, for the treatment of effluents with high sulphate loads, in particular, few studies have focused on ion removal during LDHs precipitation [19–24]. In aiming for the treatment of acid mine drainages through specific sulphate removal, no work has been reported to date [25].

Observing the lack of data referring to the treatment of sulphate-rich effluents using LDHs in specific literature, the present work proposes a new route for sulphate ion removal focusing on acid mine drainages. This procedure comprises the precipitation of a Layer Double Hydroxide (LDH) composed of Mg^{2+} and Al^{3+} with NO_3^- and SO_4^{2-} anions located in the interlayer space. It is an operationally simple process, as any precipitation process, but presents the advantage of (i) leaving residual sulphate concentrations lower than the most traditional precipitation process (via gypsum formation) for this anion removal; and (ii) can be applied in a wide pH range (from 4 to 12), which cannot be done by the ettringite process of sulphate removal.

2. Experimental

2.1. Sulphate ion removal by the precipitation of a LDH comprising Mg^{2+} and Al^{3+} in batch and continuous systems using synthetic solutions and wastewater

The experiments for sulphate removal from aqueous solutions were carried out in batch and continuous systems. In both the cases, individual solutions containing nitrate salts of magnesium ($Mg(NO_3)_2$; 8200 mg(Mg^{2+}) L^{-1}) and aluminium ($Al(NO_3)_3$; 3100 mg(AL^{3+}) L^{-1}) were mixed with a sodium sulphate (Na_2SO_4; 5400 mg(SO_4^{2-}) L^{-1}) solution in equal volumes. These solutions were prepared to ensure concentrations of Mg^{2+}, Al^{3+} and SO_4^{2-} ions, respectively, 2700, 1030 and 1800 mg L^{-1} in the reaction medium. The experimentally applied sulphate concentration was an average of the values frequently reported in studies concerning the treatment of acid mining drainages [5,25,26]. The Mg^{2+} and Al^{3+} concentrations were then selected according to the stoichiometric proportion for the formation of $Mg_6Al_2(SO_4)(OH)_{16}.nH_2O$ LDH-like compound, using the sulphate concentration as reference.

For the batch experiments, a 50 mL aliquot of each of the above mentioned individual solutions ($Mg(NO_3)_2$, $Al(NO_3)_3$ and Na_2SO_4) were mixed in a 250 mL Erlenmeyer flask. The pH was kept at 2, 4, 6, 8, 10 and 12 during the entire experiment (from 30 min to 8 h) and was adjusted every 30 min either using nitric acid or sodium hydroxide solutions. During the experiments, the Erlenmeyer flasks were stirred at 150 min^{-1} in a temperature-controlled shaker (*New Brunswick Scientific*, "*Inova* 44") at 35 °C, 50 °C and 70 °C. At the end of these experiments, the solid-solution pulp was filtered and the solid samples were dried at 50 °C for approximately 24 h then stored in a desiccator. The liquid fractions were directed to chemical analysis. The wide pH and temperature ranges adopted experimentally were chosen in order to evaluate with greater accuracy the effect of the respective parameters on the present studied precipitation process.

In the continuous experiments, the $Mg(NO_3)_2$, $Al(NO_3)_3$ and Na_2SO_4 solutions were separately pumped at a constant flow rate (8 ± 0.5 mL min^{-1} for each solution) into a cylindrical reactor of 10 cm in diameter and 600 mL of total capacity. The system was constantly stirred at 200 min^{-1} using a suspended-mechanical stirrer *(Ika)* at 26 ± 1 °C. The pH inside the reactor was set at 10 ± 0.5 using a sodium hydroxide solution, which was fed to the system at a flow rate of 2 ± 0.5 mL min^{-1} throughout the experiment. The pulp filled approximately 260 mL of the reactor capacity. Every 10 min, a 100 mL sample was collected and filtered. The solid phase was dried as described in Section 2.1 and subsequently directed to analyses along with the liquid samples.

Continuous experiments were also carried out using a sulphate-rich wastewater sample from Minas Gerais, Brazil. The methodology was the same described in the experiments carried out with synthetic solutions (item 2.1). However, instead of using a sodium sulphate solution, the wastewater (containing 1903.8 mg L^{-1} of sulphate and having pH 6) was the sulphate source. In addition, these experiments were performed without any pH adjustment. The sulphate removal efficiency was evaluated using the WHO recommendations as reference, which recommends that the maximum sulphate concentration in water for human consumption has to be less than 500 mg L^{-1} [4,6].

2.2. Material and solution characterisation

The magnesium, aluminium and sulphur concentrations of the liquid samples produced during the experiments were determined by ICP/OES (*Varian/Agilent*, 725-ES). Subsequently, the sulphur contents were mathematically converted into sulphate concentration.

The morphological characteristics were investigated using a scanning electron microscope attached to an energy dispersive spectrometer (*Tescan, VEGA 3 LMH)* with an accelerating voltage of 20 kV for the sample surfaces coated with gold. In addition, the carbon and sulphur contents of the solid samples were analysed in an *LECO* analyser (model *SC632*).

The crystalline solid phases were also analysed in an X-ray diffractometer *(PanAnalytical, Empirean)* equipped with a copper tube, which was operated at 40 mA and 45 kV. The scanning was performed between 2° and 70° in 0.02°/2θ steps, every 40 s. The diffractograms obtained were compared to the patterns published by the *International Committee of Diffraction Data* (ICDD) database.

Infrared spectra in the medium region (from 400 cm^{-1} to 4000 cm^{-1}) were produced by the transmission technique in a *Thermo Electron* device, model *Nicolet 6700*, equipped with a deuterated lanthanum triglycine sulphate detector sealed with caesium iodide. The samples were mixed with approximately 1% in mass of potassium bromide, and the analysis was carried out under nitrogen atmosphere.

Thermal analysis was performed in a *Mettler Toledo* device, model *TGA/DSC 1 Star System.* The solid sample was heated in an alumina crucible in the temperature range from 25 °C to 1100 °C at a heating rate of 10 °C min^{-1} under nitrogen atmosphere (99.999%) with a flow rate of 60 mL min^{-1}.

3. Results and discussion

3.1. Characterisation of solids formed during batch and continuous experiments

3.1.1. X-ray diffraction

Figs. 1 and 2 present the diffractograms of the solid materials formed during the experiments carried out in both batch and continuous systems, respectively. As can be seen in Figs. 1 and 2, with the exception of solids produced in the experiments at pH 4, all the other samples presented crystallinity whose peaks positions showed a similar profile. However, no record was found in the ICDD database to assign to the diffractograms.

Although the samples could not be identified by X-ray diffraction, according to Forano et al. [23], the diffractograms presented in Figs. 1(b–e) and 2 (a–b) show typical basal reflections of LDH-like compounds. Thus, it is possible to affirm that this type of compound was formed in batch-wise (pH 6–12) and in continuous system using both synthetic solution and wastewater but it is not possible to say which kind of LDH the precipitated solid is, basing only on their diffractograms.

Moreover, according to Fig. 1, the samples generated in batch experiments at pH 8, 10 and 12 (Fig. 1(c–e)) presented higher crystallinity than those produced in batch-wise at pH 6 and in the continuous

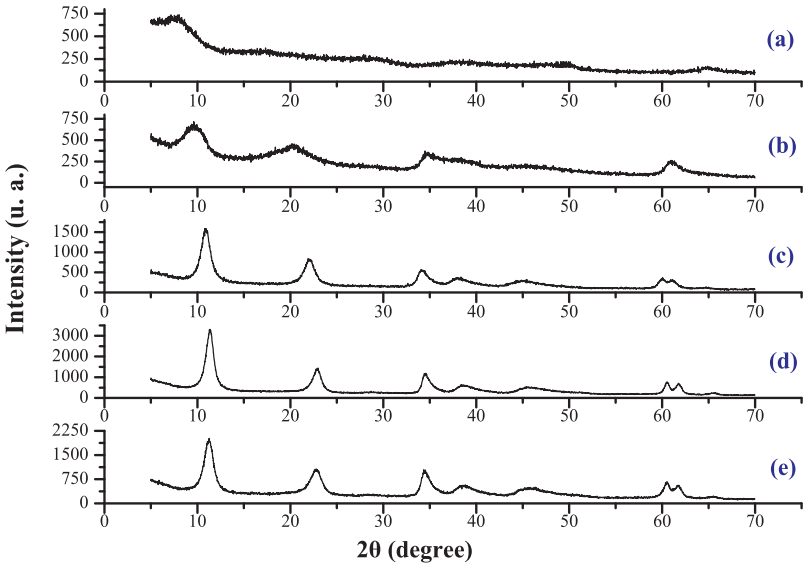

Fig. 1. X-ray diffractograms of the solids formed in the experiments carried out in batch-wise, using synthetic solution, at pH 4 (a), 6 (b), 8 (c), 10 (d) and 12.

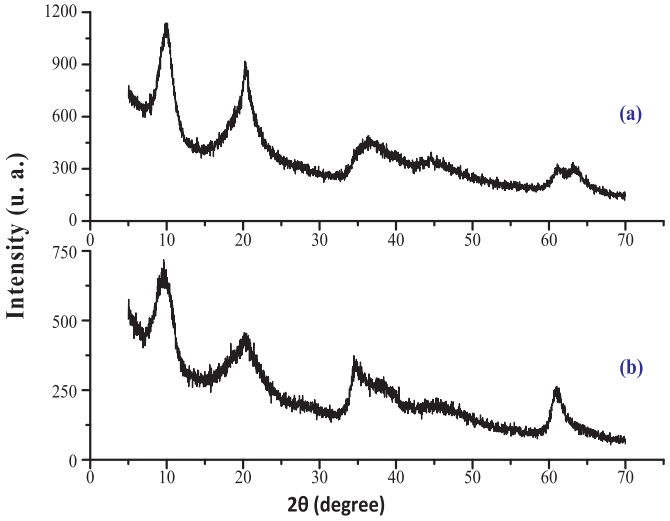

Fig. 2. X-ray diffractograms of the solids precipitated in the experiments carried out in continuous system with synthetic solution (a) and (b) wastewater.

experiments (Fig. 1(b) and 2). In general, it can be suggested that the low crystallinity observed in Fig. 2(b) happens because of the composition of the wastewater. The different ions in the solution may have co-precipitated with Mg^{2+}, Al^{3+} and SO_4^{2-}, resulting in changes of the crystalline structure of the experimentally precipitated solid. Another factor that may justify the low crystallinity of the solids formed in the continuous experiments is the short residence time adopted in those experiments, which did not favour the crystallisation kinetics of the LDH under study [27]. In this case, the time was not enough for the crystals to grow.

In the ICDD database, no record was found of the diffraction data produced in the current work. However, the diffractograms presented in Fig. 1(b–e) and 2 show typical basal reflections of LDHs-like compounds [17]. Thus, it is possible to affirm that this type of compound was formed in batch-wise, at pH 6, 8, 10 e 12, and in continuous system but is not possible to say which kind of LDH is, basing only in their diffractograms.

The *hkl* reflections of the solid formed in batch-wise tests (Fig. 1(d)) are listed in Table 1 with the respective basal spacing, the relative intensities according to the height of the main peak and the features of each reflection, which were assigned according to Forano et al. [23] and Cavani et al. [28]. By analysing the 006 and 009 planes, it can be observed that such planes presented low relative intensities [17]. This fact may have been caused by a disorder of sulphate and nitrate anions and water molecules located in the interlayer region as well as failures in the arrangement of the Mg^{2+} and Al^{3+} hydroxide layers [29]. The interlayer distance of the experimentally formed LDH (8.04 Å; basal spacing referring to the 003 plane) was slightly lower than that expected for the LDH intercalated with SO_4^{2-} (from 8.80 Å to 8.58 Å) or by NO_3^- (8.79 Å) [30]. This fact may be related to the excess of water molecules in the interlayer region [31].

3.1.2. Fourier-transform infrared (FTIR) spectroscopy and elemental analysis

As the solid samples obtained in the experiments carried out at pH 6, 8, 10 and 12 presented similar diffractograms profile, only the samples produced batch-wise under the following conditions were submitted to FTIR spectroscopy: 35 °C, pH 10 and 5 h of experiment. The respective FTIR spectrum is presented in Fig. 3. This sample was randomly chosen among those obtained in batch-wise at pH 6, 8, 10 and 12. In Fig. 3, the broad peak located in the region between 3750 cm^{-1} and 3250 cm^{-1} is assigned to the metal bound to hydroxyl groups. Another peak is seen at 1637 cm^{-1}, which is assigned to the hydroxyl structurally bonded to water, whereas the peak at 1116 cm^{-1} is typical of a sulphate S—O bond. Finally, the two peaks positioned at 656 and 555 cm^{-1} are ascribed, respectively, to Al—O and Mg—O bonds [17–32].

The peak located at 1384 cm^{-1} could be also assigned to both C—O bonds and N—O bonds since nitrate anions were added to the system from the salts source of Mg^{2+} e Al^{3+} and the dissolution of carbonate anions in alkaline media is difficult to avoid [33]. Nevertheless, the elemental analysis of carbon performed with the sample in the study did not detect this element. Thus, the possibility of this peak attributed to C—O bonds was discharged and the intense and well-defined peaks at 1384 cm^{-1}, as well as a smaller one at 831 cm^{-1}, were associated with an asymmetrically NO_3 stretching vibration.

As the presence of NO_3^- was detected during the FTIR analysis and was present in high concentration in the solution, it can be suggested that the Mg- and Al -LDHs were probably stabilised by both sulphate and nitrate anions.

3.1.3. Scanning electron microscopy and energy dispersive spectroscopy

The images obtained by the scanning electron microscopy of the solids generated in the sulphate removal process (batch-wise, pH 10,

Table 1
Reflections (*hkl*) observed on diffractogram presented on Fig. 1(d), along with their respective position, basal spacing, relative intensity in relation to the height of the main peak and characteristics.

Reflections (hkl)	Position (2θ)	Basal spacing (Å)	Relative intensity (%)	Characteristics
003	10.99	8.04	100.0	Stacking of the layers of double hydroxides and the water molecules arrangement in the interlayer region.
006	22.14	4.01	27.0	
009	34.54	2.59	22.1	
015	38.52	2.34	8.9	Ordering of each layer in relation to each other.
018	45.55	1.99	9.5	
110	60.34	1.53	15.1	Arrangement of the structure inside the layers
113	61.51	1.50	11.7	

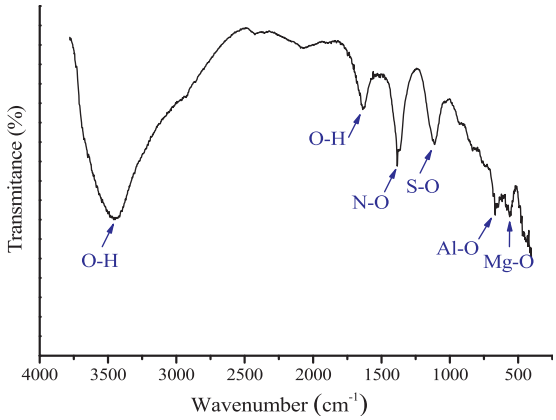

Fig. 3. FTIR spectrum of the solid samples produced in the batchwise experiments with synthetic solutions (at pH 10, 35 °C and 5 h of duration).

35 °C and 5 h of experiment), along with the respective mapping of the main elements in the sample are presented in Fig. 4. As for the FTIR analysis, this sample was randomly chosen among those obtained in batch-wise at pH 6, 8, 10 and 12. The sample has a tabular aspect (Fig. 4(a)), which is characteristic of LDHs [17,27]. In addition, the energy dispersive spectroscopy (EDS) analysis confirmed that the main elements are magnesium, aluminium, oxygen and sulphur, which are equally distributed in the sample forming a single solid phase (Fig. 4(b)).

The LDH composition estimated by the EDS analysis for the elements magnesium, aluminium and sulphur was converted to mass proportion using the magnesium percentage as a comparison parameter. These data are shown in Table 2, along with the respective theoretical values expected for a $Mg_6Al_2(SO_4)(OH)_{16}.nH_2O$-like compound. As observed in Table 2, the precipitated LDH presents the expected stoichiometric mass proportion in terms of the proportion of magnesium and aluminium. However, the sulphur percentage is below the expected value, i.e. the solid contains only half of the theoretical sulphur content, i.e. 2.7%. The sulphur content estimated by EDS analysis was confirmed by the *LECO* analysis which indicated 2.4% sulphur in the sample. Based on these data, it is suggested that the chemical formula of the LDH is probably $Mg_6Al_2((SO_4)_{(0.5)},(NO_3)_{(y)})(OH)_{12}.nH_2O$, in which y represents the molar content of NO_3 ion content in the LDH structure, which varies according to the content of positive charges non-stabilised by the sulphate ions.

Table 2
Mass proportion of the elements Mg, Al and S and their respective theoretical values expected in the LDH $Mg_6Al_2(SO_4)(OH)_{16}.nH_2O$-like compound and the experimental data obtained in the present work.

Mass Proportion	Mg^{2+}	Al^{3+}	SO_4^{2-}	Ratio Mg^{2+}/Al^{3+}
Theoretical	1.00	0.37	0.66	2.70
Estimated by EDS	1.00	0.41	0.33	2.44

3.1.4. Thermal analysis

Fig. 5 presents the curves of the thermogravimetric analysis (TG), the derivative thermogravimetry (DTG) and the differential scanning calorimetry (DSC) produced during the thermal decomposition of the solid formed in the batch-wise sulphate removal experiments of the present work. As for the FTIR analysis and SEM-EDS, the sample

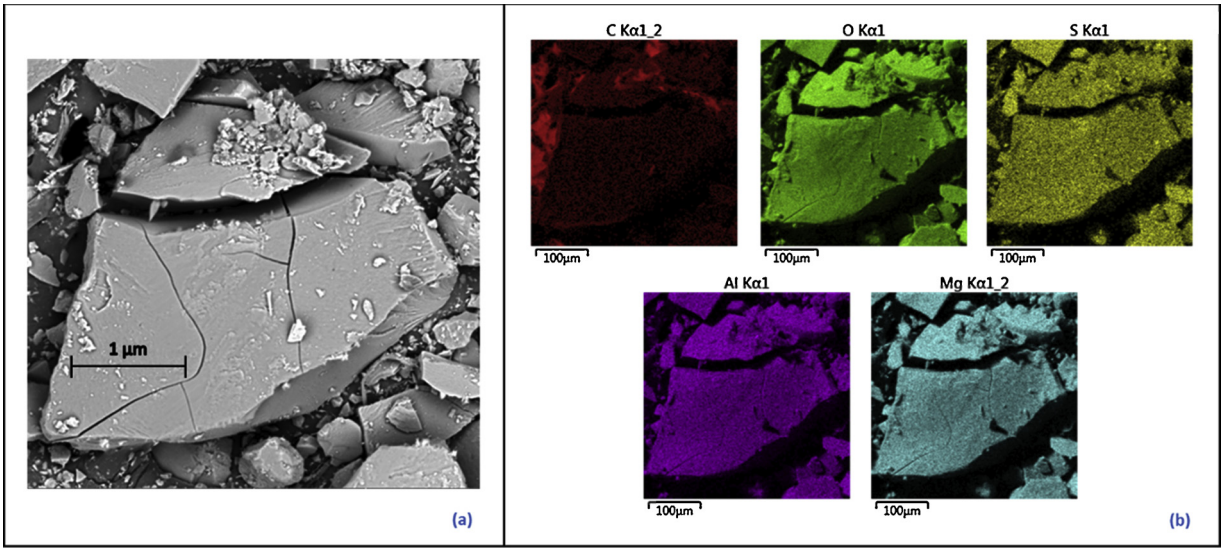

Fig. 4. Scanning electron microscopy of the solid produced in the batchwise (synthetic solution, pH 10, 35 °C and 5 h of experiment) on sulphate removal experiment (a) and with along the mappings of the main elements presented in the sample (b).

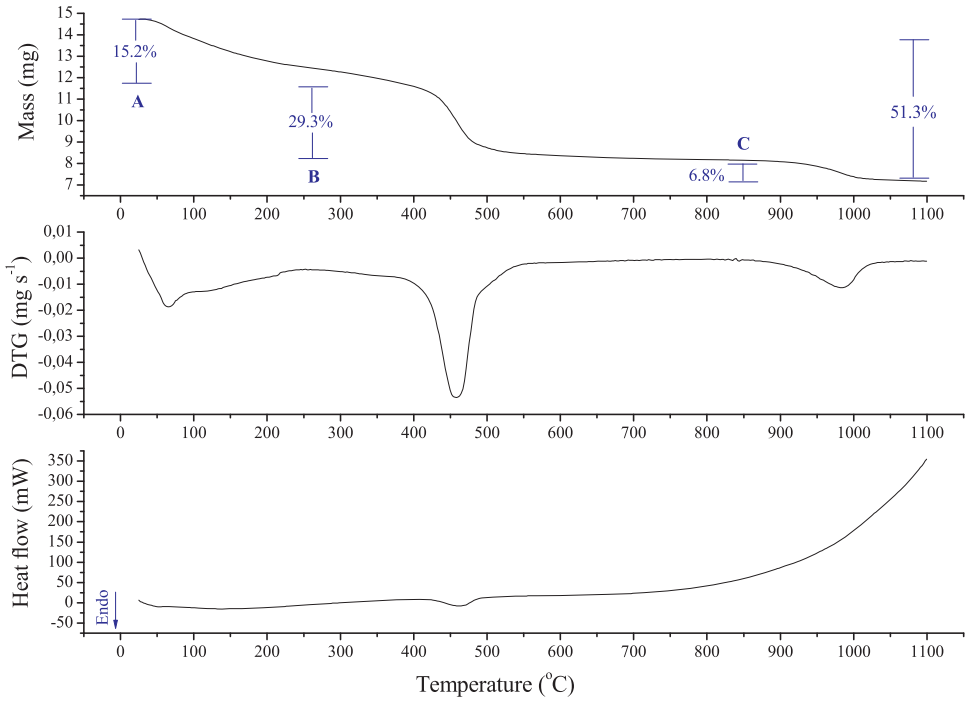

Fig. 5. TG (a), DTG (b) and DSC (c) of the solid produced in the batchwise sulphate removal process, using synthetic solution at pH 10, 35 °C and 5 h of experiment.

Table 3
Thermal events (A, B and C) occurred during heating from 25 °C to 1100 °C of the solids generated in the sulphate removal process.

Event	Temperature range (°C)	Maximum temperature (°C)	Loss mass (%)
A	25–253	64	15.2
B	253–802	458	29.3
C	802–1100	983	6.8
Total mass loss			51.3

destined to thermal analysis was randomly chosen among those obtained in batch-wise at pH 6, 8, 10 and 12. As can be seen in Fig. 5, three endothermic events (identified as A, B and C) were observed when heating the sample from 25 °C to 1100 °C. All these events indicated a mass loss with a total reduction of 51.3% in the initial mass of the sample. Table 3 presents (i) the temperature ranges in which each event occurred, (ii) the respective maximum temperatures, (iii) the mass loss relative to each event and the chemical phenomenon accounting for the mass loss.

By individually analysing these thermal events, it can be observed that the mass loss occurring during event A (15.2%), which occurred between 25 °C and 253 °C, may be credited to the loss of both adsorbed water and water molecules bonded to the double hydroxide layers in the interlayer region [34–37]. The second event involved a mass loss of 29.3% and is related to two simultaneous phenomena. The first is the decomposition of the NO_3^- groups releasing NO_2 gas [38], while the second is related to the decomposition of hydroxyl groups located in the Mg^{2+} and Al^{3+} double hydroxide layers [34–37]. As these two phenomena simultaneously occur in the temperature range from 250 °C to 800 °C, their peaks were not sufficiently resolved to enable a precise assessment of the respective water and nitrate mass percentages.

Event C, which occurred from 802 °C to 1100 °C, can be assigned to the decomposition of SO_4 groups located in interlayer region of the LDH precipitated during the experiments of the current work. This phenomenon is responsible for the formation of double oxides of Mg^{2+} and Al^{3+} as well as the release of SO_2 and O_2 gases [36,37], which justifies the mass loss that occurred during the event (6.8%). By assuming that all the SO_4 groups were decomposed in the temperature range from 802 °C to 1100 °C, it can be postulated that the sulphur content of the solid sample was 2.3%, which is equivalent to 6.8% of sulphate. Therefore, this data confirms the values given by the *LECO* analyser.

3.2. Sulphate removal from aqueous solutions by the precipitation of a LDH composed of Mg^{2+} and Al^{3+}

3.2.1. Batch experiments

Fig. 6(a) and (b) represent the final Mg^{2+}, Al^{3+} and SO_4^{2-} concentrations and their respective removal efficiencies observed as a function of the reaction time. As can be seen in Fig. 6(a), the proposed sulphate removal process requires 1 h to reach approximately 450 mg L^{-1} residual sulphate concentration, which corresponds to 75% removal, whereas the aluminium and magnesium removals are practically 100% for the same period (Fig. 6(b)). Such outcome leads to the conclusion that the proposed process is fast and slightly influenced by the mixing time of the precipitating agents used in the experiment. This characteristic may be a consequence of the high affinity of the sulphate ions and the layers of double hydroxide of Mg^{2+} and Al^{3+}. Usually, the nucleation kinetics is fast, and the crystal growth process, on the other hand, is slow [27]. The experimentally observed sulphate removal yields are comparable with those achieved during ettringite and gypsum precipitations, which are the most applied processes in the industry for the same purpose. Studies that investigated the effect of reaction time on sulphate removal through precipitation of such compounds reported a maximum removal in up to two hours [13,29].

Upon assessing the effect of temperature, a strong influence of this parameter in the sulphate removal efficiency was not observed (Fig. 7(a) and (b)). The experiments carried out between 35 °C and 70 °C showed that an average value of 78% of the sulphate ions initially presented in the medium was removed. Usually, during LDHs precipitation, a temperature increase up to about 80 °C results in the formation of crystalline phases with larger particle sizes [27,39]. The small influence of temperature in industrial sulphate removal processes was also observed in studies aiming for ettringite precipitation [15].

Although both mixing time and temperature did not interfere in the LDH precipitation, acidity must be controlled because high sulphate removals (~75%) were observed only in the experiments in which the

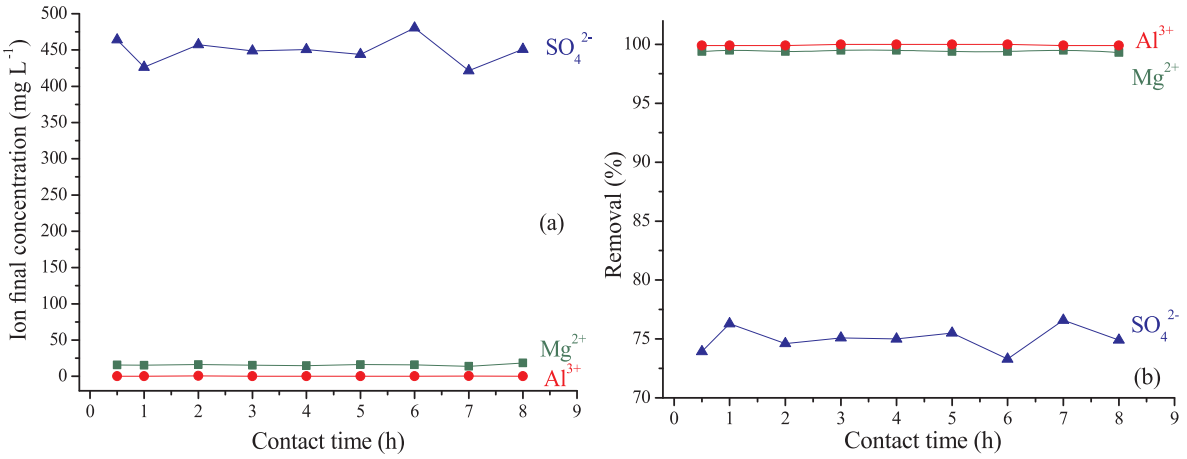

Fig. 6. Effect of time on the final Mg^{2+}, Al^{3+} and SO_4^{2-} concentrations (a) and the associate removal efficiencies (b) observed in the batchwise experiments. Initial concentrations in the system (total volume = 150 mL): SO_4^{2-} = 1800 mg L^{-1}, Mg^{2+} = 2700 mg L^{-1} and Al^{3+} = 1010 mg L^{-1}, 35 °C, pH = 10 and 150 min^{-1}. NO_3- concentrations were not determined.

pH of the solution was equal to or above 4, according to Fig. 8(a) and (b). As there was no solid formation at pH 2, consequently, no anion removal was observed. Therefore, the pH must be controlled to ensure the formation of the proposed LDH. Above pH 4, the sulphate removal efficiency became independent of this parameter. This result is consistent with the literature [30,35,40], which states that pH interferes with the stability of LDH-like compounds. The data reported in the current study also revealed that the proposed procedure is innovative because about of 75% of sulphate removal may be promoted in a wide range of pH (from 4 to 12), with an initial concentration of 1800 mg L^{-1}. Among the most industrially applied methods to remove sulphate from liquid effluents, ettringite precipitation is only feasible in highly alkaline mediums (pH around 11) [12,15,33], whereas gypsum precipitation, although feasible in a wide range of pH, always produces a residual sulphate concentration above 1200 mg L^{-1} in the aqueous medium [7,29,33,41,42].

To summarise, the observed characteristics of the sulphate removal process in batch-wise that was proposed in the current work suggest new positive aspects with regard to a potential industrial application as it: (i) is fast, (ii) is slightly influenced by temperature, (iii) may be applied over a wide range of pH (4–12) without affecting the anion removal efficiency (~75%), which was the same in all studied conditions of temperature and pH, (iv) results in negligible residual Mg^{2+} and Al^{3+} content, and (v) produces a residual sulphate concentration which complies with the WHO recommendations (i.e. 500 mg L^{-1} maximum) [6].

3.2.2. *Experiments in continuous systems using both synthetic solutions and wastewater samples*

The sulphate removal data achieved in the continuous experiments using the synthetic solution and the wastewater are presented in Figs. 9 and 10, respectively. As presented in Fig. 9(a), the experiments with the synthetic solution reached the steady-state condition after four residence times (40 min). When assessing the test, whose sulphate source was wastewater, three residence times (30 min) were necessary for the steady state to be attained (Fig. 10(a)).

At the steady state, the experiments performed in the continuous system with the synthetic solution showed sulphate removal similar to that observed in the batch experiments, i.e. around 75% removal (Figs. 6–9). However, the sulphate removal was higher, i.e. between 85% and 90% (Fig. 9(b)), in the experiments with wastewater. The higher sulphate removal efficiency observed may be related to the excess of aluminium and magnesium in relation to the sulphate quantity present in the aqueous media in the test performed with the wastewater. With the wastewater, the sulphate concentration was initially 630 mg(SO_4^{2-}) L^{-1}, in the test with the synthetic solution, the sulphate concentration was 1800 mg(SO_4^{2-}) L^{-1}. Conversely, in both conditions (batch and continuous systems), around 1030 mg L^{-1} of Al^{3+} and

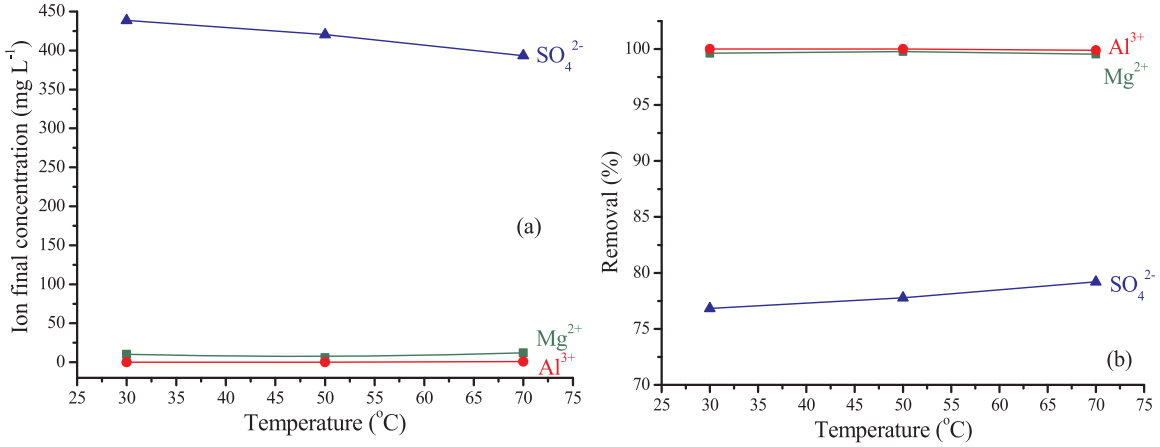

Fig. 7. Effect of temperature on the final Mg^{2+}, Al^{3+} and SO_4^{2-} concentrations (a) and the associate removal efficiencies (b) observed in the batchwise experiments carried out in 5 h of experiment, at pH = 10 and stirring rate of 150 min^{-1}. Initial concentrations in the system (total volume = 150 mL): SO_4^{2-} = 1800 mg L^{-1}, Mg^{2+} = 2700 mg L^{-1} and Al^{3+} = 1010 mg L^{-1}. NO_3- concentrations were not determined.

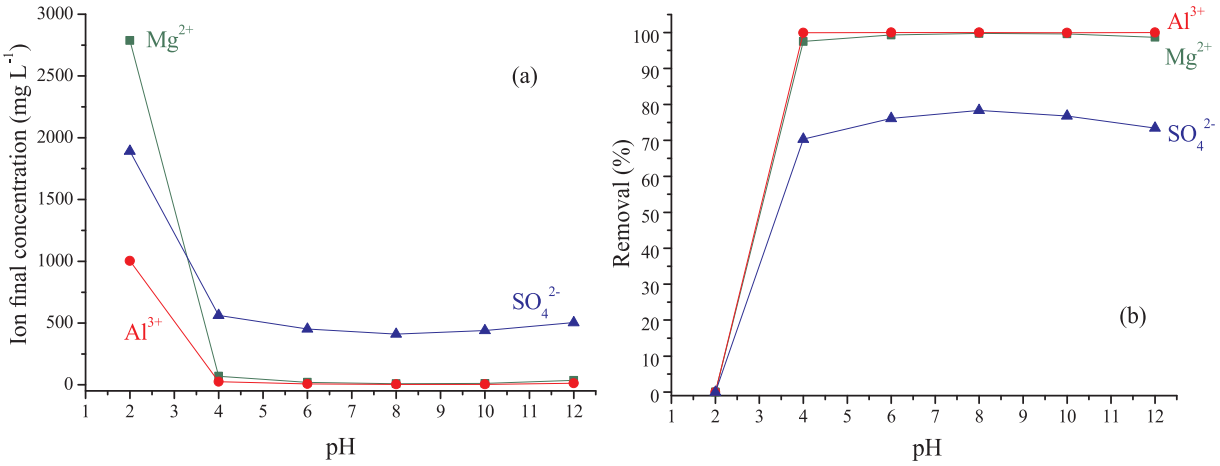

Fig. 8. Effect of pH on the final Mg^{2+}, Al^{3+} and SO_4^{2-} concentrations (a) and the associate removal efficiencies (b) observed in the batchwise experiments carried out at 35 °C and stirring rate of 150 min^{-1} during 5 h. Initial concentrations in the system (total volume = 150 mL): SO_4^{2-} = 1800 mg L^{-1}, Mg^{2+} = 2700 mg L^{-1} and Al^{3+} = 1010 mg L^{-1}. NO_3- concentrations were not determined.

2700 mg L^{-1} of Mg^{2+} was made available in the aqueous medium (item 2.1). It is important to mention that although the original sulphate concentration of the wastewater was equal to 1903.8 mg L^{-1}, this concentration was diluted three times because equal volumes of the wastewater, $Mg(NO_3)_2$ and $Al(NO_3)_3$ solutions simultaneously entered the reactor. In experiments performed under conditions similar to those of the present study, Ferreira et al. [15] investigated sulphate precipitation from synthetic solutions (1654 mg(SO_4^{2-}) L^{-1}) by promoting ettringite precipitation. In this study, a removal of about 85% of the anion was observed, which corresponded to a residual sulphate concentration of approximately 250 mg L^{-1}.

Contrary to what was observed in the batch-wise tests, the residual Mg^{2+} concentration in the effluent of the continuous experiment was 250 mg L^{-1} (Fig. 9(a)) when a synthetic sodium sulphate solution was utilised, whereas the concentration was approximately 450 mg L^{-1} (Fig. 10(a)) when the wastewater sample was utilised. This may be caused by the different residence times adopted in both types of experiments (batch and continuous). Therefore, longer continuous experiments should be performed in order to achieve lower residual concentrations of Mg^{2+}.

The residual aluminium concentrations were lower than the limit of detection of aluminium (2 mg L^{-1}) in both batch and continuous tests, using both synthetic solution and wastewater. This accounts for an interesting characteristic of this process since aluminium is a toxic element that can cause adverse neurobehavioral changes and lung fibrosis. Studies also suggest that aluminium can induce reproductive system toxicity, teratogenicity and autism spectrum disorder [43].

Although the proposed precipitation process has resulted in residual concentration of Mg^{2+}, Al^{3+} and SO_4^{2-} ions that is in accordance to the recommendations established by WHO [4,6], from the point of view of effluent disposal, it is important to mention that the use of nitrate salts as a source of magnesium and aluminium contributed to the generation of a final effluent rich in nitrate. Therefore, it is suggested that future studies be conducted using the combination of different sources of aluminium and magnesium, such as hydroxides, chlorides and chlorates. Only the use of their respective carbonates is not recommended because, according to Forano et al. [23], the carbonate ion has considerably higher affinity for the layers of double hydroxide higher than the sulphate ions. Thus, the presence of carbonate anion in the aqueous solution could decrease the efficiency of the proposed sulphate precipitation process.

In general, as observed in the experiments performed in a batch-wise and in a continuous system, the proposed process also presented positive characteristics to its further industrial application since it: (i) is also fast, (ii) is feasible at pH 6 (which is not possible with ettringite precipitation process) and (iii) results in residual Mg^{2+}, Al^{3+} and SO_4^{2-} content in accordance with the WHO recommendations [4,6].

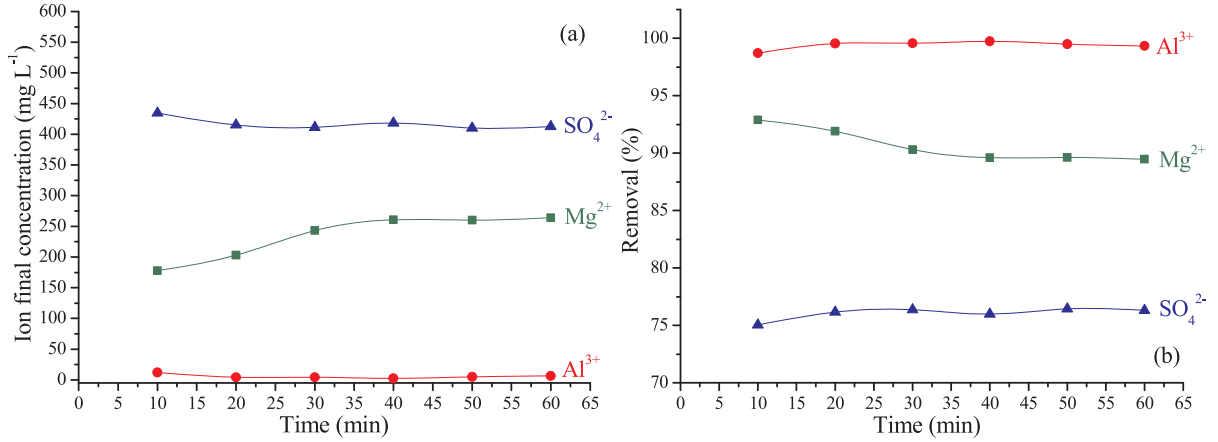

Fig. 9. Final Mg^{2+}, Al^{3+} and SO_4^{2-} concentrations (a) and the associate removal efficiencies (b) observed in the continuous experiments using synthetic solution (Temperature = 26 ± 1 °C; pH = 6; Residence time: 10 min). NO_3- concentrations were not determined.

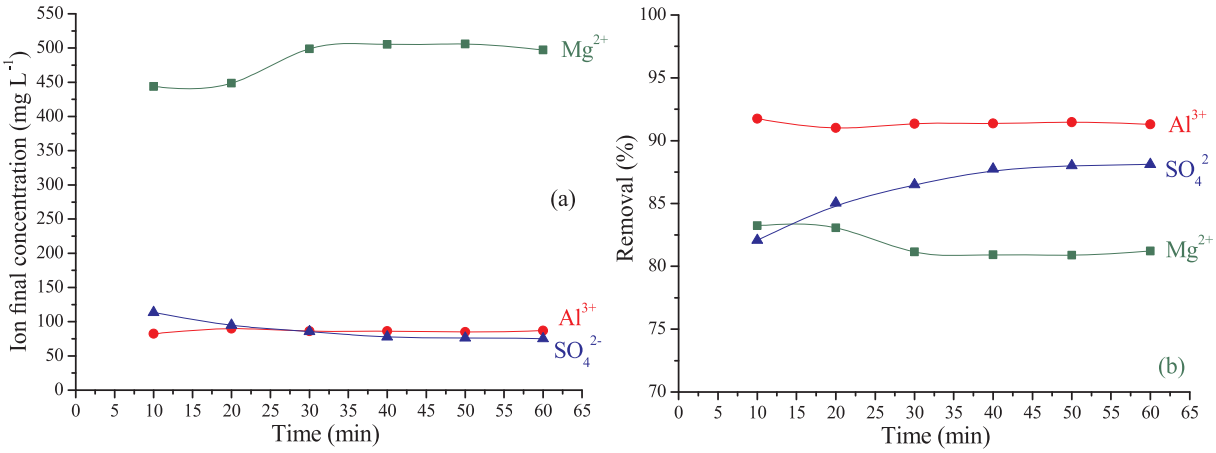

Fig. 10. Final Mg^{2+}, Al^{3+} and SO_4^{2-} concentrations (a) and the associate removal efficiencies (b) observed in the continuous experiments using an industrial wastewater (Temperature = 26 ± 1 °C; pH = 6; Residence time: 10 min). NO_3- concentrations were not determined.

4. Conclusions

A new alternative route for sulphate removal from aqueous solutions was developed in the current work. Through that, about 75% sulphate removal was observed from a synthetic solution containing an initial sulphate concentration of 1800 mg L^{-1}. Approximately 90% removal efficiency was verified in experiments with industrial wastewater samples, which initially contained 630 mg(SO_4^{2-}) L^{-1} in the system. Comparing the proposed precipitation process with the routes currently applied industrially, i.e. ettringite and gypsum precipitation, the procedure proposed in the present work is innovative since its efficiency of sulphate removal is practically the same within a wide range of pH values (from 4 to 12). In addition, this process is operationally simple, fast and its sulphate efficiency removal is also slightly influenced by temperature (from 30 °C to 70 °C). The solid precipitated in this process at pH 6–12 is an LDH composed of Mg^{2+} and Al^{3+} and intercalated with SO_4^{2-} and NO_3^- ($Mg_6Al_2((SO_4)_{0.5},(NO_3)_y)(OH)_{12}.nH_2O$). The formation of this type of LDH has not been reported yet in the context of wastewater treatment, neither for sulphate nor for nitrate removal. In this latter case, further studies are required as well as an investigation about the interfering anions that could be present in aqueous media.

Acknowledgements

Financial support was received from the funding agencies FINEP, FAPEMIG, CNPq and CAPES, and the characterisation analyses was performed by UFOP's Laboratories of Thermal Analysis, Thermal Treatment, X-ray Diffraction and the Hydrometallurgy Laboratory at UFMG are greatly appreciated.

References

[1] G.S. Simate, S. Ndlovu, Acid mine drainage: challenges and opportunities, J. Environ. Chem. Eng. 2 (2014) 1785–1803.
[2] K.K. Kefeni, T.A.M. Msagati, B.B. Mamba, Acid mine drainage: prevention, treatment options, and resource recovery: a review, J. Clean. Prod. 151 (2017) 475–493.
[3] INAP, International Network for Acid Prevention: Treatment of Sulphate in Mine Effluents - Lorax Environmental, (2003).
[4] WHO, Sulfate in Drinking Water – Background for Development of WHO Guidelines for Drinking Water Quality, Genebra (2004).
[5] H. Runtti, E.T. Tolonen, S. Tuomikoski, T. Luukkonen, U. Lassia, How to tackle the stringent sulfate removal requirements in mine water treatment—a review of potential methods, Environ. Res. 167 (2018) 207–222.
[6] WHO, Guidelines for Drinking-Water Quality, 4th edition, World Health Organization, Geneva, 2011.
[7] I. Doye, J. Duchesne, Neutralisation of acid mine drainage with alkaline industrial residues: laboratory investigation using batch-leaching tests, Appl. Geochem. 18 (2003) 1197–1213.
[8] A.J. Geldenhyus, J.P. Maree, M. Beer, P. Hlabela, An integrated limestone/lime process for partial sulfate removal, J. South Afr. Inst. Min. Metall. 103 (2003) 345–354.
[9] S.S. Potgieter-Vermaak, J.H. Potgieter, P. Monama, R. Van Grieken, Comparison of limestone, dolomite and fly ash as pre-treatment agents for acid mine drainage, Miner. Eng. 19 (2006) 454–462.
[10] E.T. Tolonen, J. Ramo, U. Lassi, The effect of magnesium on partial sulphate removal from mine water as gypsum, J. Environ. Manage. 159 (2015) 143–146.
[11] G. Kaur, S.J. Couperthwaite, B.W. Hatton-Jones, G.J. Millar, Alternative neutralisation materials for acid mine drainage treatment, J. Water Process. Eng. 22 (2018) 46–58.
[12] E. Álvarez-Ayuso, H.W. Nugteren, Synthesis of ettringite: a way to deal with the acid wastewaters of aluminium anodising industry, Water Res. 39 (2005) 65–72.
[13] R. Silva, L. Cadorin, J. Rubio, Sulphate ions removal from an aqueous solution: I. Co-precipitation with hydrolysed aluminum-bearing salts, Miner. Eng. 23 (2010) 1220–1226.
[14] G. Madzivire, L.F. Petrik, W.M. Gitari, T.V. Ojumu, G. Balfour, Application of coal fly ash to circumneutral mine waters for the removal of sulphates as gypsum and ettringite, Miner. Eng. 23 (2010) 252–257.
[15] B.C.S. Ferreira, R.M.F. Lima, V.A. Leão, Remoção de sulfato de efluentes industriais por precipitação, Engenharia Sanitária e Ambiental 16 (2011) 1–8.
[16] W. Dou, Z. Zhou, L.M. Jiang, A. Jiang, R. Huang, X. Tian, W. Zhang, D. Chen, Sulfate removal from wastewater using ettringite precipitation: magnesium ion inhibition and process optimization, J. Environ. Manage. 196 (2017) 518–526.
[17] K.H. Goh, T.T. Lim, Z. Dong, Application of layered double hydroxides for removal of oxyanions: a review, Water Res. 42 (2008) 1343–1368.
[18] K. Grover, S. Komarneni, H. Katsuki, Synthetic hydrotalcite-type and hydrocalumite-type layered double hydroxides for arsenate uptake, Appl. Clay Sci. 48 (2010) 631–637.
[19] S. Paikaray, M.J. Hendry, J. Essilfie-Dughan, Controls on arsenate, molybdate, and selenate uptake by hydrotalcite-like layered double hydroxides, Chem. Geol. 345 (2013) 130–138.
[20] F.L. Theiss, S.J. Couperthwaite, G.A. Ayoko, R.L. Frost, A review of the removal of anions and oxyanions of the halogen elements from aqueous solution by layered double hydroxides, J. Colloid Interface Sci. 417 (2014) 356–368.
[21] L. Deng, Z. Shi, Synthesis and characterization of a novel Mg–Al hydrotalcite-loaded kaolin clay and its adsorption properties for phosphate in aqueous solution, J. Alloys Compd. 637 (2015) 188–196.
[22] B. Kostura, R. Škuta, D. Plachá, J. Kukutschová, D. Matýsek, Mg–Al–CO3 hydrotalcite removal of persistent organic disruptor—nonylphenol from aqueous solutions, Appl. Clay Sci. 114 (2015) 234–238.
[23] C. Forano, T. Hibino, F. Leroux, C. Taviot-Guého, Chapter 13.1. Layered double hydroxides, Dev. Clay Sci. 1 (2006) 1021–1095.
[24] E. Alvarez-Ayuso, H.W. Nugteren, Emission reduction of aluminium anodising industry by production of Mg2+-Al3+-SO4(2-)-hydrotalcite-type compound, Chemosphere 62 (2006) 155–162.
[25] W.A.M. Fernando, I.M.S.K. Ilankoona, T.H. Syeda, M. Yellishetty, Challenges and opportunities in the removal of sulphate ions in contaminated mine water: a review, Miner. Eng. 117 (2018) 74–90.
[26] INAP, International Network for Acid Prevention: Global Acid Rock Drainage Guide, (2009).
[27] A.A. Eliseev, A.V. Lukashin, A.A. Vertegel, V.P. Tarasov, Y.D. Tret'yakov, A study of crystallization of Mg–Al double hydroxides, Dokl. Chem. 387 (2002) 777–781.
[28] F. Cavani, F. Trifirò, A. Vaccari, Hydrotalcite-type anionic clays: preparation, properties and applications, Catal. Today 11 (1991) 173–301.
[29] S. Tait, W.P. Clarke, J. Keller, D.J. Batstone, Removal of sulfate from high-strength wastewater by crystallization, Water Res. 43 (2009) 762–772.
[30] S. Miyata, Anion-exchange properties of hydrotalcite like compounds, Clays Clay Miner. 31 (1983) 305–311.
[31] W. Feitknecht, On the alpha-form of hydroxide divalent metals, Helv. Chim. Acta 21 (1938) 766–784.
[32] S.J. Hug, In situ Fourier transform infrared measurements of sulfate adsorption on

hematite in aqueous solutions, J. Colloid Interface Sci. 188 (1997) 415–422.
[33] D. Guimarães, V.A. Oliveira, V.L. Leão, Kinetic and thermal decomposition of ettringite synthesized from aqueous solutions, J. Therm. Anal. Calorim. 123 (2016) 1–11.
[34] V.R.L. Constantino, T.J. Pinnavaia, Basic properties of Mg2+1-x, AI3+, layered double hydroxides intercalated by carbonate, hydroxide, chloride, and sulfate anions, Inorg. Chem. 34 (1995) 883–892.
[35] S. Miyata, A. Okada, Synthesis of hydrotalcite like compounds and their physicochemical properties the systems Mg2+-Al3+-SO42- and Mg2+-Al3+-CrO42-, Clays Clays Miner. 25 (1977) 14–18.
[36] R.L. Frost, K.L. Erickson, Decomposition of the synthetic hydrotalcites mountkeithite and honessite—a high resolution thermogravimetric analysis and infrared emission spectroscopic study, Thermochim. Acta 421 (2004) 51–58.
[37] R.L. Frost, A.W. Musumeci, T. Bostrom, M.O. Adebajo, M.L. Weier, W. Martens, Thermal decomposition of hydrotalcite with chromate, molybdate or sulphate in the interlayer, Thermochim. Acta 429 (2005) 179–187.
[38] C. Ribeiro, Intercalação de ânion Enalaprilato em hidróxido duplo lamelar recoberto com xiloglucana: estudos de liberação in vitro, Universidade Federal do Paraná, 2008, p. 79.
[39] K. Hosni, E. Srasra, Simplified synthesis of layered double hydroxide using a natural source of magnesium, Appl. Clay Sci. 43 (2009) 415–419.
[40] S. Miyata, Physico-chemical properties of synthetic hydrotalcites in relation to composition, Clays Clay Miner. 28 (1980) 50–56.
[41] J.P. Maree, P. Du Plessis, C.J. Van Der Walt, Treatment of acidic effluents with limestone instead of lime, Water Sci. Technol. 26 (1992) 345–355.
[42] J.P. Maree, P. Du Plessis, Neutralisation of acid mine water with calcium carbonate, Water Sci. Technol. 26 (1994) 285–296.
[43] R.A. Yokel, The toxicology of aluminum in the brain: a review, Neurotoxicology (2016) 122–127.